Journal of Hazardous Materials 181 (2010) 633–639

Contents lists available at ScienceDirect

Journal of Hazardous Materials

journal homepage: www.elsevier.com/locate/jhazmat

Ruthenium versus platinum on cerium materials in wet air oxidation of acetic acid

J. Gaálová [a], J. Barbier Jr. [b,*], S. Rossignol [c]

[a] Institute of Chemical Process Fundamentals of the CAS, Rozvojová 135, 165 02 Prague 6, CZ
[b] University of Poitiers, LACCO UMR 6503, Laboratoire de Catalyse par les Métaux, 40 Avenue du Recteur Pineau, F-86022 POITIERS Cedex, France
[c] University of Limoges, ENSCI, 47 Avenue Albert Thomas 87000 Limoges France

ARTICLE INFO

Article history:
Received 26 February 2010
Received in revised form 12 May 2010
Accepted 13 May 2010
Available online 21 May 2010

Keywords:
Ruthenium
CWAO
Ceria
mixed oxide
Deactivation

ABSTRACT

This study was a comparison between Ru-catalysts and similar, previously investigated, Pt-catalysts. In this paper, ruthenium catalysts for catalytic wet air oxidation are prepared, characterized and tested. Both catalysts were supported on commercial CeO_2 as well as mixed oxide $Zr_{0.1}(Ce_{0.75}Pr_{0.25})_{0.9}O_2$. The catalysts were characterized by measuring the oxygen storage capacities (OSC), BET, XRD, FTIR and chemisorption of hydrogen. In addition, the effect of sintering (treatments under H_2) was compared with both of the catalysts. The comparison of the results showed that initial intrinsic activity of ruthenium is not significantly influenced by the type of the support, which is contrast to platinum. Furthermore, the particle size of Ru had an important effect on CWAO activity: the higher the particle size, the better the activity. This was different with Pt-catalysts, where the optimal particle size was smaller, having about 15% of metal dispersion.

1. Introduction

The aim of the study was to compare the prepared Ru-catalysts with similar, previously prepared and tested Pt-catalysts [1]. Wet air oxidation (WAO) is one of the several processes of water treatments with a medium chemical oxygen demand ($5 < COD < 150$ g L^{-1}). Under conventional reaction conditions, one of the essential steps in the reaction pathway corresponds to the oxygen transfer [2]. Thus, the study of different noble metal catalysts [3–8], have been focused on cerium-based heterogeneous catalysts [9–12], due to their high oxygen storage capacity and oxygen mobility [13–16].

Many studies have been performed on the cerium-based heterogeneous catalysts in wet air oxidation of acetic acid [17–19] and the rate determining step for CWAO of various organic compounds [20–22].

In our research, we focused on CWAO of acid acetic catalyzed by platinum or ruthenium supported on cerium based materials. First approach to compare these two metals has been previously demonstrated [23]. It was shown that both nature and particle size of noble metal determine activity of catalysts. In our earlier studies, the metal particule size of Pt catalyst was optimized. It was shown that the carbonaceous species formation can be limited and thus the activity improved by optimizing the metal particle size [1]. This article deals with new ruthenium homologues (1.25 wt.-%) of those platinum catalysts, supported on commercial CeO_2 as well as on mixed oxide $Zr_{0.1}(Ce_{0.75}Pr_{0.25})_{0.9}O_2$. The main objective of the research was to investigate the analogous influence of metal particle size on CWAO of acetic acid using various characterization techniques before and after catalytic reaction tests for ruthenium. The complete study permits to observe the differences between platinum and ruthenium supported on ceria-based materials in CWAO of acetic acid and to reveal new findings concerning the role of metal and support or their interface.

2. Experimental

2.1. Catalyst preparation

Table 1 presents the supports as well as their abbreviations. Cerium oxide is commercial Rare Earth ceria HSA 5 delivered by Rhodia. The support $Zr_{0.1}(Ce_{0.75}Pr_{0.25})_{0.9}O_2$ was prepared by sol-gel method, according to previously reported procedure [24], using cerium (III), praseodymium (III) nitrate and zirconium n-propoxide as precursors. Both supports were calcined under static air for 5 h at 800 °C. The treatment was the same as in the case of platinum supports prepared earlier [1].

The catalysts were prepared in a rotating evaporator by impregnation and dry evaporation of 4.938 g of the support with 9.8 cm^3 of aqueous solution of $RuCl_3$ (6.3 g_{Ru} L^{-1}) completed with HCl solution (0.150 mol L^{-1}) to 30 cm^3 (8 cm^3_{sol} $g_{support}^{-1}$). The concentration of

* Corresponding author. Tel.: +33 0 5 49 45 48 31; fax: +33 0 5 49 45 37 41.
E-mail address: Jacques.barbier.jr@univ-poitiers.fr (J. Barbier Jr.).

0304-3894/$ – see front matter © 2010 Elsevier B.V. All rights reserved.
doi:10.1016/j.jhazmat.2010.05.059

Table 1
Abbreviations of the supports and the 1.25 wt.-% ruthenium catalysts (reduced at four different temperatures: 350, 500, 650 and 800 °C).

Oxide support	Abbreviations	
	Supports	Ru catalysts reduced at different T (°C)
CeO_2*	Ce	RuCe_350, RuCe_500, RuCe_650, RuCe_800
$Zr_{0.1}(Ce_{0.75}Pr_{0.25})_{0.9}O_2$	ZrCePr	RuZrCePr_350, RuZrCePr_500, RuZrCePr_650, RuZrCePr_800

* commercial Rhodia Rare Earth ceria HSA 5.

the solution was calculated to obtain a metal content of 1.25 wt.-% (pH = 1). As in the case of platinum catalysts [1], it corresponds to 124 $\mu mol_{Met}\ g^{-1}$. The samples were dried overnight at 120 °C and finally activated by reduction under H_2 (0.33 $cm^3\ s^{-1}$) for 3 h at 350, 500, 650 and 800 °C in order to obtain different dispersion values of ruthenium (Table 1).

2.2. CWAO

Catalytic wet air oxidation experiments were carried out in 0.44 L Hastelloy C22 autoclave. The basic reaction conditions were: T = 200 °C, P_{O2} = 2 MPa, volume of acetic acid solution = 0.16 L, COD = 5 g L^{-1}, catalyst loading 4 g L^{-1}. All details concerning the apparatus, reaction conditions and experimental runs are described in ref. [1]. From the results, molar ratio of mineralization, initial specific activity and turn over frequency were calculated for each experiment. The mineralization molar ratio M (Eq. 1) corresponds to the ratio of the total CO_2 formed in CWAO ([CO_2] in mmolC.L^{-1}) and the total initial amount of organic carbon (TOC_i in mmolC.L^{-1}).

$$M = \frac{[CO_2]}{TOC_i} \quad (1)$$

CO_2 is formed according to the Eq. 2.

$$CH_3COOH + 2O_2 \rightarrow 2CO_2 + 2H_2O \quad (2)$$

The initial specific activity (A) is the amount of CO_2 formed during the first hour of reaction per gram of metal (mmol $CO_2.g_{Me}{}^{-1}.h^{-1}$) (Eq. 3),

$$A = \frac{100.(M_{1h} - M_{blank1h}).[acetic]_i.2}{m_{Cata}.w_{Me}} \quad (3)$$

where $[acetic]_i$ is the initial concentration of pollutant (in mmol.L^{-1}), 2 the number of C atoms in CH_3COOH, w_{Me} the wt.-% of metal and m_{cata} the mass of catalyst per liter. The calculation of A is obtained after deduction of the mineralization molar ratio at 1 hour for the blank experiment ($M_{blank1h}$, on bare support).

Turn over frequency (TOF (s^{-1})) or the initial intrinsic activity is calculated from Eq. 4.

$$TOF = \frac{A.M_{Me}}{36000.D} \quad (4)$$

In this equation, M_{Me} is the molar weight of metal and D the metal dispersion (in %).

We retrieve that:

- compared to the initial pollutant concentration (0.078 mol L^{-1}) under these reaction conditions, oxygen in the solution is initially in deficient proportion but remains constant all along the run by the liquid/gas equilibrium (about 0.020 mol L^{-1}).
- Only product of CWAO of acetic acid is CO_2.

2.3. Catalyst characterizations

The specific surface areas of the samples were determined from the nitrogen adsorption isotherms at −196 °C in an automated Micromeritics Tristar 3000 apparatus after evacuation for 2 h at 250 °C using a simple BET 7-point procedure at a P/P_0 ratio of 0.05–0.25. The complete adsorption and desorption isotherms have been obtained for few samples, leading to information about porous volume.

Diffractograms and particle sizes were determined by XRD experiments using a Siemens D 5005 powder θ–θ diffractometer using $Cu_{K\alpha}$ radiation ($\lambda_{K\alpha}$ = 0.154186 nm) and a graphite back-monochromator. The XRD patterns were obtained under the following conditions: dwell time, 2 s; step, 0.04° or 0.02°; constant divergence slit, 1°. Particle phases were identified by comparison with Powder Diffraction File standards from ICDD. The average particle sizes (d) were calculated using Scherrer's equation, described previously [1]. The most intense diffraction peak of ruthenium (101) displays, as in the case of platinum catalysts, an intensity too low to calculate precisely the particle size; therefore, the average sizes of ruthenium particles were determined in addition by hydrogen chemisorption.

Metal dispersions of the catalysts were estimated by hydrogen chemisorption in a chromatographic microreactor at −85 °C. Hydrogen pulses (0.26 cm^3) were injected at regular intervals after reduction under H_2 (350 °C, 3600 s) and degassing under argon (350 °C, 10800 s) using ultra-pure H_2 and Ar (<1 ppm impurities). To calculate the particle sizes of ruthenium (d in nm) using the cubic model, the surface of Ru per mol (S_{Me}) is 46.95 $m^2\ mol^{-1}$ and the metal density (ρ_{Me}) is 12.37 g cm^{-3}. [25]

The measurement of oxygen storage capacities (OSC) of the samples was also described in detail in reference [1]. The only difference here is the OSC of metal (OSC_{Me}). Total Ru oxidation into RuO_2 gives following Eq. 5:

$$OSC_{Me} = 2.\frac{10^4\ .\ w_{Me}}{M_{Me}} = 248\ \mu mol\ g^{-1} \quad (5)$$

where w_{Me} is the weight of metal per gram of catalyst and M_{Me} the molar weight of metal.

FT-IR spectra were collected using a Perkin–Elmer spectrometer. The powder sample (10 mg) was dispersed on KBr (150 mg). Experimental conditions were as follows: acquisition time, 120 s; number of scans, 20; resolution, 4 cm^{-1}.

The cubic cell parameters for the supports are: a_{Ce} = 0.554138 nm and a_{ZrCePr} = 0.53913 nm [1].

3. Results

3.1. Metal - support interaction

The structural properties of new ruthenium catalysts are shown in Table 2. In accordance with literature data [26], if the particle surface area is measured by BET, the particles seem to be more agglomerated than when the calculation is based on cubic model from XRD spectra. The BET surface areas and particle sizes of catalytic materials after deposition of ruthenium do not differ significantly from those of bare supports, reported previously [1]. Fig. 1 permits to compare specific surface area ratio of ruthenium and platinum catalysts as a function of reduction temperature. It shows clearly that the values remain stable for ruthenium materials, but decrease at higher reduction temperature for platinum samples, especially when the metal is initially well dispersed on Ce.

Table 2
BET surface area, support particle size (d_{sup}), dispersion (D) and Ru particle size (d_{Ru}) for all samples.

Samples	BET ($m^2\ g^{-1}$)	d_{sup} [a] (nm)	D [b] (%)	d_{Ru} [c] (nm)
RuCe_350	44	16	5	19
RuCe_500	41	16	5	19
RuCe_650	42	16	5	19
RuCe_800	42	17	1	94
RuZrCePr_350	21	17	9	10
RuZrCePr_500	21	17	6	16
RuZrCePr_650	21	17	2	47
RuZrCePr_800	20	19	1	94

[a] determined by XRD measurements, (estimated relative standard deviation: +/- 10%)
[b] H_2 chemisorption measurements [25] (estimated relative standard deviation: +/- 5%)
[c] determined by H_2 chemisorptions.

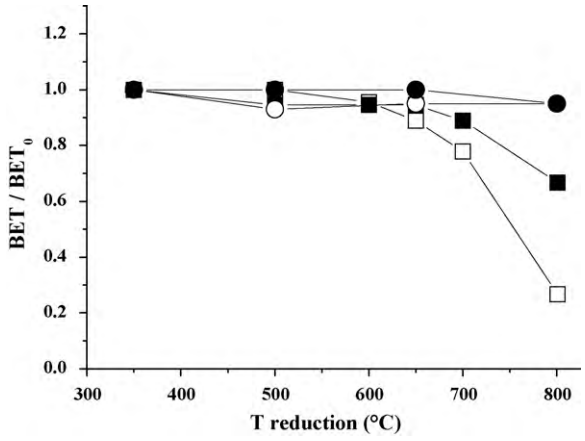

Fig. 1. Specific surface area ratio as a function of reduction temperature for the various 1.25 wt.-% ruthenium catalysts (spheres) and their platinum homologues (squares) [1] impregnated on Ce (empty symbols) and ZrCePr (full symbols) supports.

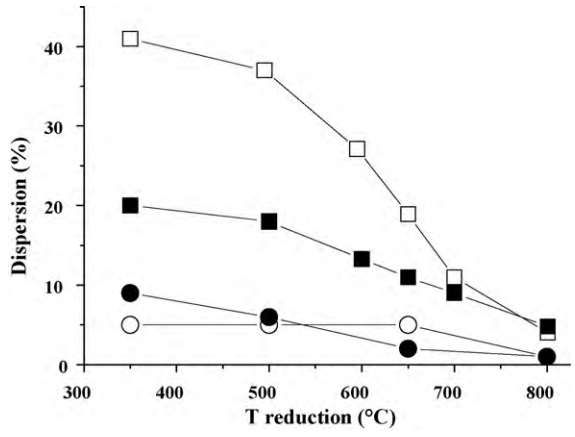

Fig. 2. Metal dispersion as a function of reduction temperature for various 1.25 wt.-% ruthenium catalysts (spheres) and their platinum homologues (squares) [1] impregnated on Ce (empty symbols) and ZrCePr (full symbols) supports.

Fig. 2 illustrates the values of metal dispersion as a function of reduction temperature for ruthenium catalysts and, in purpose of comparison, for platinum catalysts from [1]. A more wide range of dispersion was obtained for platinum than for ruthenium, especially on pure cerium oxide. The conditions of impregnation, in term of pH, are different between the two metals; acidic medium for Ru salt $[RuCl_6]^{3-}$ and basic for platinum one $[Pt(NH_3)_4]^{2+}$. Moreover,

Table 3
OSC values and number of oxygen layers (NL) for all samples.

Sample	OSC ($\mu mol\ g^{-1}$) (accuracy (+/- 5%))			NL
	measured[a]	support[b]	surface[c]	
RuCe_350	484	236	223	1.06
RuCe_500	466	218	232	0.94
RuCe_650	487	239	237	1.01
RuCe_800	498	250	238	1.05
RuZrCePr_350	952	704	107	6.58
RuZrCePr_500	844	596	107	5.57
RuZrCePr_650	862	614	107	5.74
RuZrCePr_800	850	602	97	6.22

[a] OSC measured at 400 °C
[b] $OSC_{sup} = OSC_{meas} - OSC_{Me}$
[c] theoretical number of reducible surface oxygen atoms.

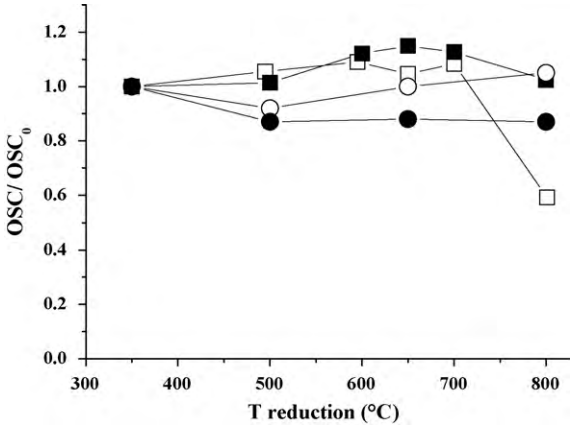

Fig. 3. Oxygen storage capacity ratio as a function of reduction temperature for the various 1.25 wt.-% ruthenium catalysts (spheres) and their platinum homologues (squares) [1] impregnated on Ce (empty symbols) and ZrCePr (full symbols) supports.

in those pH conditions the number and nature of adsorption sites are different [27], which induce dissimilar dispersion between Pt and Ru catalysts.

3.2. Oxygen storage capacity

OSC values and calculated number of oxygen atoms layers involved in the OSC process (NL) for all ruthenium samples are reported in Table 3. Oxygen storage capacity values are, as in the case of platinum catalysts [1], much higher for mixed oxides than for pure ceria and the bulk oxygen atoms are involved in the process of O_2 transfer (NL > 1). NL values remain near 1 for the noble metals supported on pure cerium oxide. The oxygen storage capacity ratio is reported as a function of reduction temperature for the various 1.25 wt.-% ruthenium catalysts on the Fig. 3 and compared to their platinum homologues [1]. Similarly to the specific surface areas, the values remain relatively stable until the highest reduction temperature of the ruthenium catalysts, but start to decrease at 800 °C for platinum supported on cerium oxide.

3.3. Catalytic test

The Fig. 4 shows the mineralization curves of acetic acid versus time for the Ru catalysts deposited on the two supports. Only the samples reduced at the two extreme temperatures (350 and 800 °C) are presented here. The catalytic activities are compared to those obtained without metal (blank experiment). The initial reaction rate of RuCe_350 is the most important and the mineralization curves of Ce catalysts begin to flatten after 2 hours of reaction,

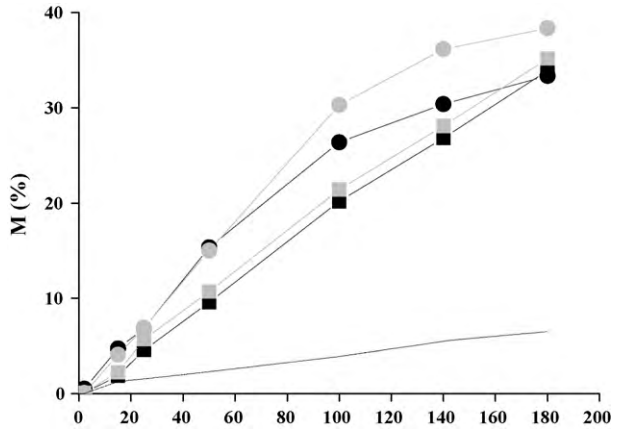

Fig. 4. Mineralization percentage as a function of time for —●— RuCe_350, —●— RuCe_800, —■— RuZrCePr_350, —■— RuZrCePr_800 catalysts and ····· Ce650, ZrCe500 or ZrCePr650 supports.

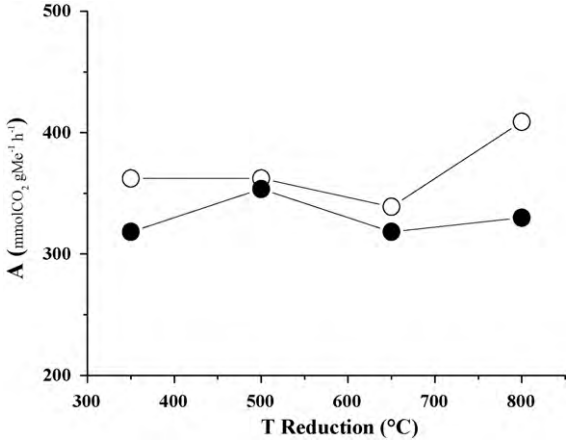

Fig. 5. Initial specific activity of ruthenium catalysts for acetic acid CWAO versus reduction temperature for ruthenium catalysts on —○— Ce and —●— ZrCePr supports.

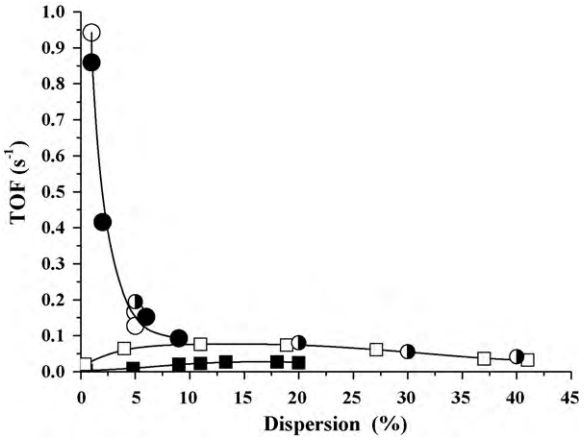

Fig. 6. TOF as a function of dispersion (from Table 2) for 1.25 wt.-% ruthenium catalysts (spheres) and their platinum homologues (squares) from ref. [1] impregnated on Ce (empty symbols) and ZrCePr (full symbols) supports. Added dots ◑ correspond to results obtained from ref. [5].

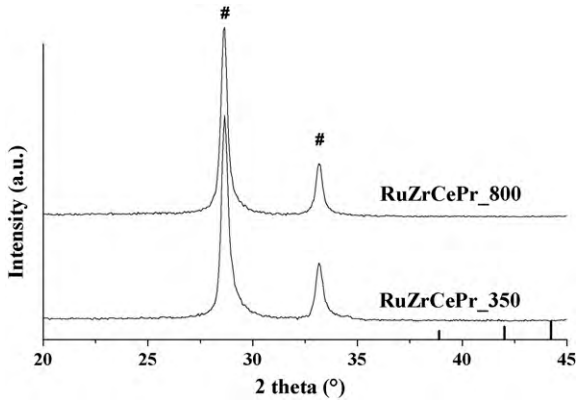

Fig. 7. X-Ray patterns of fresh RuZrCePr catalysts (# PDF: 34-0394 CeO_2; – PDF: 06-0663 Ru°).

reflecting a deactivation of catalysts. The catalysts deposited on ZrCePr supports are less active but are more stable.

The initial specific activity (A) of studied ruthenium catalysts in acetic acid conversion (mmol $CO_2.g_{Me}{}^{-1}.h^{-1}$) was not significantly affected by the sintering of the metal (Fig. 5). To determine the initial intrinsic activity, the turn over frequencies (TOF) were calculated and reported as a function of metal dispersion shown in Fig. 6. The initial intrinsic activity of ruthenium catalysts (i) decreases strongly when the dispersion increased and (ii) is independent of the nature of the support. This result is confirmed by the added dots, from previous work [5], on well dispersed RuCe catalysts, which permit to extrapolate the curve to higher dispersions. Moreover, these additional results allow comparing platinum and ruthenium in larger scale of dispersion on ceria. On one hand, it is noticeable that both noble metal catalysts behave similarly for dispersion higher than 15%. On the other hand, at low dispersions, the comparison between platinum [1] and ruthenium reveals a fundamental difference between the two metals. The behaviours of the catalysts in term of TOF values are opposite. When large metallic particles of Pt° are quasi-inactive, the same Ru particles present very high initial intrinsic activities and the turnover frequencies are maximal on the largest particles. This result is directly linked to the difference in red-ox properties of each metal in aqueous oxygenated solution. As it was shown in previous works [5,28], the highest catalytic activity is obtained, when Ru phase remained partially in zero-valent state in the particles. The best catalyst for CWAO of acetic acid, is composed of large Ru^0 particles surrounded with Ru^{n+} species. Moreover, ruthenium III and IV species are known to be good candidates for catalyzing the production of very active superoxide radicals via reaction (6) [29,30]:

$$Ru^{3+} + O_2 \rightarrow Ru^{4+} + O_2{}^{\cdot -} \quad (6)$$

In contrast to platinum catalysts [1], over ruthenium catalysts, no direct correlation was observed between the OSC values and the turn over frequencies. Due to the partial oxidation of the surface of large ruthenium particles, the rate of oxygen transfer from the support to the metal (directly linked to the OSC values) is not a limiting step for the ruthenium catalysts. Nevertheless, smallest Ru particles are rapidly fully oxidized in less active RuO_2 form [31], which induces low TOF values for high Ru dispersions. These TOF values are similar to those obtained on well dispersed Pt°.

3.4. Post-characterizations of the catalysts

The catalysts were characterized by XRD and FT-IR before and after CWAO reaction. Only RuZrCePr catalysts present, after reaction, weak diffraction lines assigned to the formation of large crystallites of $Ce(CO_3)(OH)$ and $Pr(CO_3)(OH)$. It is why we present here only the X-ray patterns ($20° < 2\theta < 45°$) of RuZrCePr fresh (Fig. 7) and after CWAO test (Fig. 8). These catalysts are not subjected to sintering. Taking into account a higher standard potential

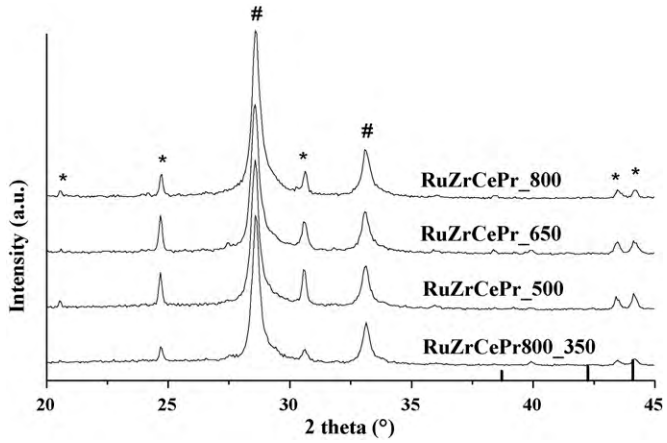

Fig. 8. X-Ray patterns of RuZrCePr catalysts after reaction (# PDF: 34-0394 CeO_2; * PDF: 52-0352 $Ce(CO_3)(OH)$ et PDF: 27-1376 $Pr(CO_3)(OH)$; | PDF: 06-0663 Ru°).

in aqueous solution of praseodymium ($E_0Pr^{4+}/Pr^{3+} = 3.2 \pm 0.2$ V) than of cerium ($E_0Ce^{4+}/Ce^{3+} = 1.7 \pm 0.1$ V) [32] and the data from HSC simulation program [33] the red-ox reaction in solid state (PrO_2, cubic):

$$2PrO_2(s) + Ce_2O_3(s) \leftrightarrows 2Pr_2O_3(s) + 2CeO_2(s) \quad (7)$$

leads to a complete forward reaction with Δ_rG° between -294 and -269 kJ mol^{-1} for temperatures in the range 0-1000 °C and consequently the formation of $Pr(CO_3)(OH)$ is favored. The mean size of these particles is in the range of 40-50 nm. Even if the particle sizes of the supports are similar after the reaction (Fig. 8), the formation of very large hydroxycarbonate crystallites points out a partial degradation of the catalyst during the experimental run. Their presence is clearly visible and appears most for the catalysts presenting a ruthenium dispersion of approximately 2-3%. This can be directly related with the higher NL values obtained by OSC measurements on the RuZrCePr catalysts. If a high mobility of the bulk oxygen atoms is demonstrated, the carbonaceous species are able to migrate into the lattice of the support and destroy it partially to form structured hydroxycarbonates. Effectively, acetic or carbonic acid present in the reaction medium (pH ≈ 4) can react directly with the support materials inducing the formation of carbonaceous species, as it was observed with platinum catalysts [34].

It was confirmed that the presence of hydroxycarbonate species seems to be responsible to an inhibition of the oxygen transfer, which strongly limited also the catalytic activities of platinum catalysts observed before [1].

Fig. 9 illustrates the FT-IR spectra of all samples before and after test. The fresh catalysts may contain surface carbonaceous species due to the ability of supporting oxides to adsorb the carbon dioxide from the atmosphere, related to their basic features. The FT-IR spectra of the fresh RuCe catalysts (Fig. 8a), do not permit to clearly identify the presence of carbonaceous species. Only the band at 1618 cm^{-1}, corresponding to the presence of adsorbed H_2O [35], is intense for Ce catalysts. The fresh RuZrCePr catalysts (Fig. 9b) are

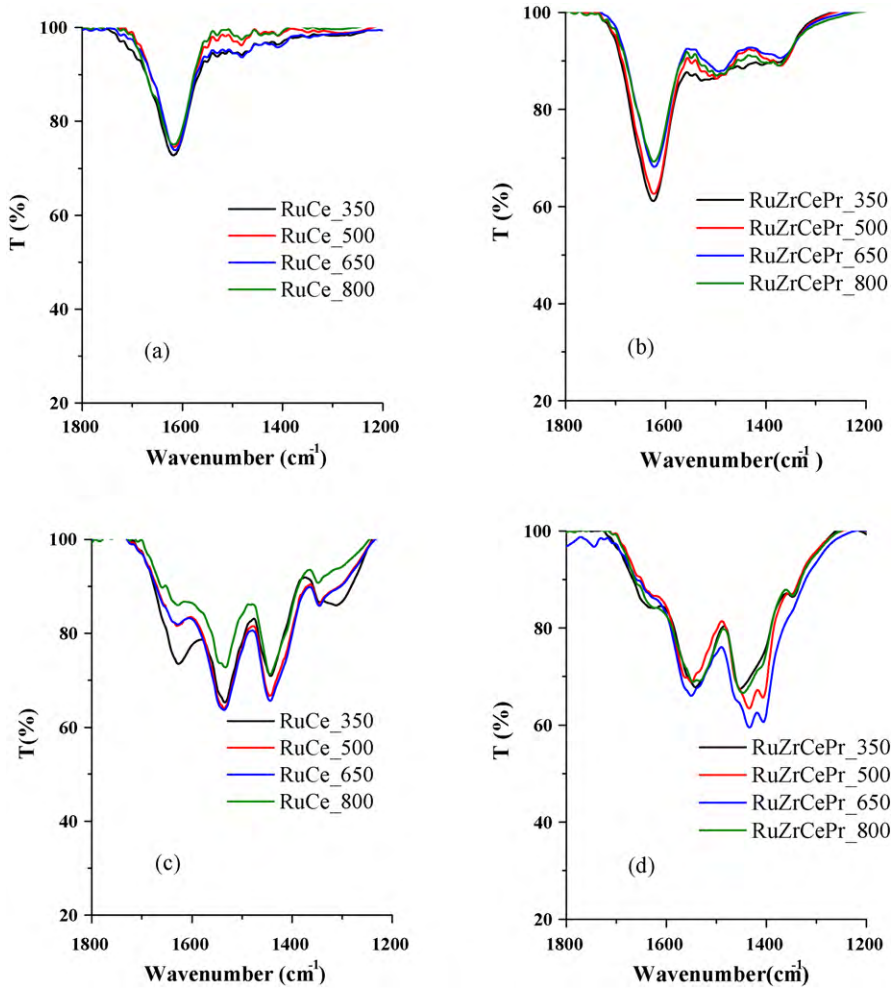

Fig. 9. Infrared spectra of RuCe (a, c), and RuZrCePr (b, d) catalysts before (a, b) and after (c, d) CWAO reaction.

more carbonated. For these catalysts, other minor species are also identified: for example monodentate carbonates (ν_{CO} = 1500 and 1370 cm^{-1}) [36]. Compared to pure ceria, a slight shift of band frequencies can be observed, that is characteristic for materials with a higher level of vacancies induced into the structure by the cations (Zr and Pr) [37].

During the reaction, several surface carbonaceous species are formed: monodentate carbonates (ν_{CO} = 1520 and 1350 cm^{-1}) and bidentate carbonates (ν_{CO} = 1550 and 1310 cm^{-1}) are present in important proportions in the case RuCe (Fig. 9c) catalysts. Polydentate carbonates (ν_{CO} = 1460, 1443 and 1410 cm^{-1}) and adsorbed water (at 1618 cm^{-1}) are observed as well. For RuZrCePr (Fig. 9d), where mono and bidentate species are comparable to those obtained on Ce, the polydentate carbonates are formed in majority. Even if these FT-IR bands give only a qualitative result, the amount of carbonaceous species appears much higher after CWAO reaction on the used RuZrCePr catalysts than for the RuCe ones. These FT-IR characterizations confirm the highest amount of carbonaceous species for the catalyst supported on ternary ZrCePr oxide which was previously demonstrated also by XRD characterization. For RuCe catalyst, where the oxygen storage capacity is limited to the surface, the carbonaceous species are essentially present at the catalyst surface after reaction. For RuZrCePr, displaying very high NL values, the carbonaceous species formation affects both, the bulk and the surface. As it was previously demonstrated [1], the evolution of carbonate amounts could be linked to the NL values of the catalysts. However, even if the amounts of carbonaceous species are higher on RuZrCePr catalysts for a given dispersion, the TOF values are very similar for the different Ru catalysts. Consequently, the inhibiting effect on catalytic activity due to a blockage of the oxygen transfer by carbonaceous species on or in the support of platinum catalysts [1] is not observed for Ru ones. Contrary to what it was observed on platinum catalysts, the nature of the support does not affect the TOF values of Ru catalysts.

In addition, concerning noble metal stability, no leaching was detected by additional ICP-MS analyses.

4. Conclusion

Catalytic wet air oxidation process is limited by the low solubility of oxygen. The influence of sintering (treatment H_2) was studied for ruthenium catalysts in order (i) to modify the oxygen transfer from the gaseous phase onto the metallic active site of the catalyst and (ii) to determine the effect of these treatments on the catalytic activity and stability (iii) to compare those results with platinum homologues previously reported [1]. It was confirmed, that the oxygen transfer from the gaseous phase to the noble metal active site is strongly improved by doping of ceria supports by Zr and Pr cations.

The sintering of ruthenium catalysts under H_2 improves the initial intrinsic activity. The higher is reducing temperature and consequently ruthenium particle size, the higher is TOF value. Even if the rate of oxygen transfer between the metal and the support does not change, it is not important anymore due to the presence of surface Ru-oxides. Ru catalyst activities are consequently independent on the nature of the tested supports which is demonstrated by the fact that the correlation between OSC and TOF values does not exist. Therefore, compared to the platinum catalysts [1], the equivalent ruthenium materials demonstrate higher resistance against poisoning by carbonaceous species during the CWAO experiments. Consequently, those catalysts are very active even if the carbonaceous species are formed during the CWAO reaction.

Acknowledgement

The authors would like to thank Pierre Emmanuel Panouillot for his help in the preparation and testing of the catalysts.

References

[1] J. Mikulová, S. Rossignol, J. Barbier Jr., D. Mesnard, D. Duprez, C. Kappenstein, Wet air oxidation of acetic acid over platinum catalysts supported on cerium based materials - Influence of metal and oxide particle sizes, J. Catal. 251 (2007) 172–181.
[2] J. Barbier Jr., L. Oliviero, B. Renard, D. Duprez, Catalytic Wet Air Oxidation of ammonia over M/CeO_2 catalysts in the treatment of Nitrogen-containing pollutants, Catal. Today 75 (2002) 29–34.
[3] J. Levec, A. Pintar, Catalytic oxidation of aqueous solutions of organics. An effective method for removal of toxic pollutants from waste waters, Catal. Today 24 (1995) 51–58.
[4] L. Oliviero, J. Barbier Jr., S. Labruquère, D. Duprez, Role of the metal-support interface in the total oxidation of carboxylic acids over Ru/CeO_2 catalysts, Catal. Lett. 60 (1999) 15–19.
[5] J. Barbier Jr., F. Delanoë, F. Jabouille, D. Duprez, G. Blanchard, P. Isnard, Total oxidation of acetic acid in aqueous solutions over noble metal catalysts, J. Catal. 177 (1998) 378–385.
[6] J. Wang, W. Zhu, S. Yang, W. Wang, Y. Zhou, Catalytic wet air oxidation of phenol with pelletized ruthenium catalysts, Appl. Catal. B: Environ. 78 (2008) 30–37.
[7] A. Cybulski, J. Trawczynski, Catalytic wet air oxidation of phenol over platinum and ruthenium catalysts, Appl. Catal. B: Environ. 47 (2004) 1–13.
[8] L. Oliviero, J. Barbier Jr., D. Duprez, Wet air oxidation of nitrogen-containing organic compounds and ammonia in aqueous media, Appl. Catal. B: Environ. 40 (2003) 163–184.
[9] B. Renard, J. Barbier Jr., D. Duprez, S. Durécu, Catalytic wet air oxidation of stearic acid on cerium oxide supported noble metal catalysts, Appl. Catal. B: Environ. 55 (2005) 1–10.
[10] I. Chen, S. Lin, C. Wang, L. Chang, J. Chang, Preparing and characterizing an optimal supported ceria catalyst for the catalytic wet air oxidation of phenol, Appl. Catal. B: Environ. 50 (2004) 49–58.
[11] S. Nousir, S. Keav, J. Barbier Jr., M. Bensitel, R. Brahmi, D. Duprez, Deactivation phenomena during Catalytic Wet Air Oxidation (CWAO) of phenol over platinum catalysts supported on ceria and ceria-zirconia mixed oxides, Appl. Catal. B: Environ. 84 (2008) 723–731.
[12] C. Milone, M. Fazio, A. Pistone, S. Galvagno, Catalytic wet air oxidation of *p*-coumaric acid on CeO_2, platinum and gold supported on CeO_2 catalysts, Appl. Catal. B: Environ. 68 (2006) 28–37.
[13] S. Imamura, Catalytic and noncatalytic wet oxidation, Ind. Eng. Chem. Res. 38 (1999) 1743–1753.
[14] A. Trovarelli, Catalysis by ceria and related materials, Catal. Rev. Sci. Eng. 38 (1996) 439–520.
[15] A. Trovarelli, C. de Leitenburg, M. Boaro, G. Dolcetti, The utilization of ceria in industrial catalysis, Catal. Today 50 (1999) 353–367.
[16] A. Trovarelli, M. Boaro, E. Rocchini, C. de Leitenburg, G. Dolcetti, Some recent developments in the characterization of ceria-based catalysts, J. Alloy Compd 323 (2001) 584–591.
[17] J. Mikulová, S. Rossignol, J. Barbier Jr., D. Duprez, C. Kappenstein, Characterizations of platinum catalysts supported on Ce, Zr, Pr-oxides and formation of carbonate species in catalytic wet air oxidation of acetic acid, Catal. Today 124 (2007) 185–190.
[18] S. Imamura, Y. Taniguchi, Y. Ikeda, S. Hosokawa, H. Kanai, H. Ando, Reduction behavior of Ru/CeO_2 catalysts and their activity for wet oxidation, React. Kinet. Catal. Lett. 76 (2002) 201–206.
[19] S. Hosokawa, H. Kanai, K. Utani, Y. Taniguchi, Y. Saito, S. Imamura, State of Ru on CeO_2 and its catalytic activity in the wet oxidation of acetic acid, Appl. Catal. B:. Environ. 45 (2003) 181–187.
[20] L. Oliviero, J. Barbier Jr., D. Duprez, H. Wahyu, J.W. Ponton, I.S. Matcalfe, D. Mantzavinos, Experimental and predictive approach for determining wet air oxidation reaction pathways in synthetic wastewaters, Appl. Catal. B: Environ. 35 (2001) 1–12.
[21] P. Gallezot, S. Chaumet, A. Perrard, P. Isnard, Catalytic wet air oxidation of acetic acid on carbon-supported ruthenium catalysts, J. Catal. 168 (1997) 104–109.
[22] H. Delvin, I. Harris, Mechanism of the oxidation of aqueous phenol with. dissolved oxygen, Ind. Eng. Chem. Fund. 23 (1984) 387–392.
[23] J. Mikulová, S. Rossignol, J. Barbier Jr., D. Mesnard, D. Duprez, C. Kappenstein, Ruthenium and platinum catalysts supported on Ce, Zr, Pr-O mixed oxides prepared by soft chemistry for acetic acid wet air oxidation, Appl. Catal. B: Environ. 72 (2007) 1–10.
[24] S. Rossignol, C. Descorme, C. Kappenstein, D. Duprez, Synthesis, structure ansd catalytic properties of Zr-Ce-Pr-O mixed oxides, J, Mater. Chem. 11 (2001) 2587–2592.
[25] D. Duprez, Les méthodes chromatographiques en catalyse hétérogène, J. Chim. Phys. 80 (1983) 487–505.
[26] T. Kobayashi, S. Iwamoto, M. Inoue, Properties of the ceria colloidal particles prepared by the solvothermal oxidation of cerium metal, J. Alloys Compd 9 (2006) 1149.
[27] D. Terribile, A. Trovarelli, J. Llorca, C. de Leitenburg, G. Dolcetti, The preparation of high surface area CeO_2–ZrO_2 mixed oxides by a surfactant-assisted approach, Catal. Today 43 (1998) 79–88.
[28] A. Pintar, J. Batista, T. Tisler, Catalytic wet-air oxidation of aqueous solutions of formic acid, acetic acid and phenol in a continuous-flow trickle-bed reactor over Ru/TiO_2 catalysts, Appl, Catal. B: Environ. 84 (2008) 30–41.
[29] C.J.M. Stirling, Radicals in Organic Chemistry, Olbourne Press, London, 1965.
[30] S. Yang, Y. Feng, J. Wan, W. Zhu, Z. Jiang, Effect of CeO_2 addition on the structure and activity of RuO_2/γ-Al_2O_3 catalyst, Appl. Surf. Sci. 246 (2005) 222–228.

[31] G. Sun, A. Xu, Y. He, M. Yang, H. Du, C. Sun, Ruthenium catalysts supported on high-surface-area zirconia for the catalytic wet oxidation of *N*,*N*-dimethyl formamide, J. Hazard. Mater. 156 (2008) 335–341.
[32] A. J. Bard, R. Parsons, J. Jordan, M. Dekker, Standard potentials in aqueous solution, Inc, New York (IUPAC) (1985) 587-629.
[33] A. Roine, "HSC chemistry ® 6.0 for windows, chemical reaction and equilibrium software with extensive thermochemical data base and flowsheet simulation.", version 5.1, Outokumpu Research Oy, Pori, Finland, (2006).
[34] C.B. Maugans, A. Akgerman, Catalytic wet oxidation of phenol in a trickle bed reactor over a Pt/TiO_2 catalyst, Water Res. 37 (2003) 319–328.
[35] Y. Sato, M. Koizumi, T. Miyao, S. Naito, The $CO–H_2$ and $CO–H_2O$ reactions over TiO_2 nanotubes filled with Pt metal nanoparticles, Catal. Today 111 (2006) 164–170 (2006).
[36] C. Binet, M. Daturi, J.-C. Lavalley, IR study of polycrystalline ceria properties in oxidised and reduced states, Catal. Today 50 (1999) 207–225.
[37] S. Rossignol, D. Mesnard, F. Gerard, C. Kappenstein, D. Duprez, Synthesis, structure and catalytic properties of Zr–Ce–Pr–O mixed oxides, J. Mater. Chem. 13 (2003) 3017–3020.